

Bis(ferrocenylethynyl)-Substituted Digold-Tetrarhenium Cluster: Unusual Structure and Electronic Communication between Ferrocenyl Groups

Avthandil A. Koridze,^{*,†,‡} Aleksey M. Sheloumov,[†] Fedor M. Dolgushin,[†] Mariam G. Ezernitskaya,[†] Edward Rosenberg,^{*,§} Ayesha Sharmin,[§] and Mauro Ravera^{*,||}

A.N. Nesmeyanov Institute of Organoelement Compounds, Russian Academy of Sciences, 28 Vavilov Street, 119991 Moscow, Russian Federation, I. Javakhishvili Tbilisi State University, 1 Chavchavadze Avenue, 380128 Tbilisi, Georgia, Department of Chemistry, University of Montana, Missoula, Montana 59812, and Dipartimento di Scienze dell'Ambiente e della Vita, Università del Piemonte Orientale "A. Avogadro", Via Bellini 25G, 15100 Alessandria, Italy

Received June 25, 2008

The digold-tetrarhenium cluster $\text{Re}_4(\text{AuPPh}_3)_2(\text{CO})_{12}(\mu_3\text{-C}\equiv\text{CFc})_2$ (**1**) was obtained by the thermolysis of known complex $\text{Re}_2(\text{AuPPh}_3)(\text{CO})_8(\mu\text{-C}\equiv\text{CFc})$ (**2**) and fully characterized by a single crystal X-ray diffraction study. Cluster **1** has a butterfly Re_4 geometry, and both Re_3 wings are capped with AuPPh_3 groups. Two ferrocenylethynyl ligands symmetrically coordinated within cavity of the wings. The dihedral angle between the Re_3 wings is rather narrow, 73.2° , whereas the 64e butterfly clusters usually have a more flattened structure. An examination of the carbonyl region of the ^{13}C NMR of **1** and **2** revealed that **1** is stereochemically rigid while **2** is fluxional with respect to a σ - π interconversion of the ferrocenyl ethynyl group across the Re – Re edge of the Re_2Au triangle. Complex **1** revealed a very rare electronic communication between the ferrocene units across the cluster core. According to the cyclic voltammetric (CV) data, cluster **1** undergoes two reversible redox process with ferrocene oxidations separated by 109 mV. Electronic communication between two ferrocene units of **1** is discussed on the basis of CV and NIR data.

Introduction

Electron transfer is pivotal to the functioning of many biological and artificial molecular devices.¹ There is great interest in developing molecular compounds for use in the construction of nanoscale electronic devices. Mixed-valence (MV) compounds can be regarded as simple systems for testing electron-transfer models.^{2–5} Essential components of these systems include the electron donor (**D**) and the acceptor (**A**) connected by a set of bonds, known as a bridge or spacer. The bridge plays a critical role in the efficiency of electron transfer, since the length, electron structure, and composition affect the electronic communication between **D** and **A**. A considerable body of work has been devoted to the investigation of connecting structures with various types of unsaturated linkages, and interesting results have been obtained with systems containing metal–metal bridges.^{2–5}

Ferrocene has excellent reversible redox properties, and with its robust (+1/0) couple, it is one of the most utilized units for

probing charge transfer across molecular fragments (**X**) on the basis of the mixed valence nature of $[\text{Fc-X-Fc}]^+$ (Fc = ferrocenyl), where in the case of efficient bridging, two Fc 's are oxidized stepwise and potential difference between two oxidations can be used as a measure of coupling strength.

In recent years, there have been intense efforts in the study of electronic communication through metal-containing fragments and clusters. To this end, ferrocenyl pendant groups are used as redox centers, and ethynylferrocene commonly serves as a starting compound.⁶ Reactions of ethynylferrocene with osmium and ruthenium cluster carbonyls were first reported by Koridze as early as in 1987 and 1992, respectively.^{7a,d} At present, there exists a number of dinuclear and cluster complexes with the ferrocenylethynyl ligand.^{7,8} However, examples of metal clusters containing chemically equivalent ferrocenyl groups are rare, and only a few of them have been structurally characterized.⁸ Well-documented examples of electron transfer within molecular frameworks containing a cluster core are rare, and in the all known compounds with two equivalent ferrocenyl groups, the metal–metal spacers do not allow significant electronic communication between ferrocene units.⁸

Herein we report the synthesis and structural characterization of $\text{Re}_4(\text{AuPPh}_3)_2(\text{CO})_{12}(\mu_3\text{-C}\equiv\text{CFc})_2$ (**1**), containing two equivalent ferrocenylethynyl groups, along with the results of electrochemical and NIR spectroscopic studies. Complex **1** revealed

* To whom correspondence should be addressed. E-mail: koridze@ineos.ac.ru; edward.rosenberg@mso.umt.edu; mauro.ravera@mfn.unipmn.it.

[†] Russian Academy of Sciences.

[‡] I. Javakhishvili Tbilisi State University.

[§] University of Montana.

^{||} Università del Piemonte Orientale "A. Avogadro".

(1) For reviews, see: (a) Astruc, D. *Acc. Chem. Res.* **1997**, *30*, 383. (b) Barlow, S.; O'Hare, D. *Chem. Rev.* **1997**, *97*, 637. (c) Demadis, K. D.; Hartshorn, C. M.; Meyer, T. G. *Chem. Rev.* **2001**, *101*, 2655. (d) Marcus, R. A. *Angew. Chem., Int. Ed. Engl.* **1993**, *32*, 111.

(2) Collier, C. P.; Wong, E. W.; Belohradsky, M.; Raymo, F. M.; Stoddart, J. F.; Kuekes, P. L.; Williams, R. S.; Heath, J. R. *Science* **1999**, *285*, 391.

(3) Robertson, N.; McGowan, C. A. *Chem. Soc. Rev.* **2003**, *32*, 96.

(4) Schenning, A.P.H.J.; Meijer, E. W. *Chem. Commun.* **2005**, 3245.

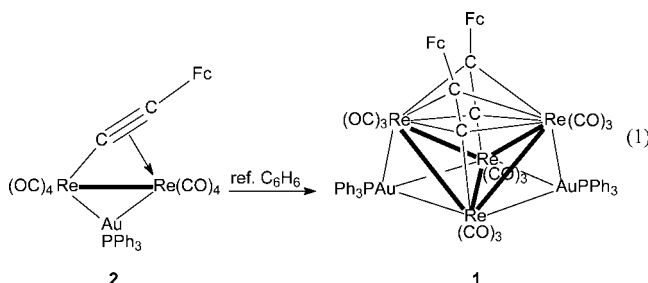
(5) Jones, S. C.; Barlow, S.; O'Hare, D. *Chem.-Eur. J.* **2005**, *11*, 4473.

(6) (a) Colbert, M. C. B.; Lewis, J.; Long, N. J.; Raithby, P. R.; White, A. J. P.; Williams, D. J. *J. Chem. Soc., Dalton. Trans.* **1997**, 99. (b) Jones, N. D.; Wolf, M. D.; Giaquinta, D. M. *Organometallics* **1997**, *16*, 1352. (c) Sato, M.; Hayashi, Y.; Kumakura, S.; Shimizu, N.; Katada, M.; Kawata, S. *Organometallics* **1996**, *15*, 721. (d) Long, N. J.; Martin, A. J.; Vilar, R.; White, A. J. P.; Williams, D. J.; Younus, M. *Organometallics* **1999**, *18*, 4261.

unusual structural features and exhibits a very rare electronic communication between two ferrocenylethynyl units which are multisite bound to the cluster backbone.

Results and Discussion

Synthesis of 1. Cluster **1** was prepared in high yield by the thermolysis of the known complex $\text{Re}_2(\text{AuPPh}_3)(\text{CO})_8(\mu\text{-C}\equiv\text{CFc})$ (**2**) (eq 1).^{7h}



The precursor of **1**, complex **2** was synthesized by the reaction of $\text{Re}_2(\text{CO})_8(\text{NCMe})_2$ with $\text{FcC}\equiv\text{CAuPPh}_3$ (**3**)^{7g} and fully characterized, including a single crystal X-ray diffraction study.^{7h} The formation of the red cluster **1** in a low yield was mentioned in this report,^{7h} but its structure remained unknown until now. Compound **1** was characterized by spectral methods. The presence of only terminal groups was evident from IR spectroscopy; the ^1H and ^{31}P NMR spectra were consistent with the presence of the ferrocenyl group and the PPh_3 ligand. It is noteworthy that, in comparison with ^1H NMR spectrum of initial complex **2** (δ 4.23 (s, 5H, C_5H_5) 4.28 (t, 2H, C_5H_4 , $J = 2.0$ Hz), and 4.58 (t, 2H, C_5H_4 , $J = 2.0$ Hz)), the resonances of the cyclopentadienyl C_5H_4 ring in **1** are substantially deshielded: δ 4.16 (s, 5H, C_5H_5) 4.55 (t, 2H, C_5H_4 , $J = 2.0$ Hz), 4.98 (t, 2H, C_5H_4 , $J = 2.0$ Hz). In the $^{31}\text{P}\{^1\text{H}\}$ NMR spectrum, a single resonance was observed at δ 90.4 ppm.

Preparation of complex **1** in high yield allowed us not only to fully characterize it by a single-crystal X-ray diffraction, but to perform a comparative electrochemical study of complexes **1**, **2**, and **3**.

X-ray Structural Determination of 1. The X-ray structure of **1** is given in Figure 1. Selected interatomic distances are listed in the Figure caption. The cluster framework of **1** shows a butterfly Re_4 geometry with the Re–Re distances adapting one normal (Re(1)–Re(2) bond 3.047(1) Å) and four elongated Re–Re bonds (3.241(1)–3.309(1) Å). For comparison, the Re–Re distance in $\text{Re}_2(\text{CO})_{10}$ ^{9a} is 3.0413(11) Å; however, there are several rhenium complexes, in which intermetallic distances significantly exceed this value. For example, in the complexes $\text{Re}_2(\mu\text{-H})(\mu\text{-Ph}_2\text{PCH}_2\text{PPh}_2)(\text{CO})_7(\eta^1\text{-C}\equiv\text{CPh})$,^{9b} $\text{Re}_2(\mu\text{-H})(\mu\text{-NC}_5\text{H}_4)(\text{CO})_8$,^{9c} and $\text{Re}_2\text{Mn}(\mu\text{-H})(\text{CO})_{14}$,^{9d} the Re–Re distances are 3.416(1), 3.2088(4), and 3.39 Å, respectively. In cluster **1**, the Re...Re distance between the wing-tip Re(3) and Re(4) atoms is significantly longer, 3.474(1) Å, than the other Re–Re distances indicating the absence of direct bonding.

In cluster **1** both wings of the Re_4 butterfly are capped with the AuPPh_3 group. The gold atoms are bound to the rhenium atoms of the Re_3 triangle in a different way, with elongated Au–Re distances for the wing-tip rhenium atoms (2.896(1) and 2.900(1) Å), and Au–Re distances for the hinge rhenium atoms ranging from 2.823(1) to 2.860(1) Å. These bond lengths are similar to those found in $[\text{Re}_3(\mu\text{-H})_3(\mu_3\text{-AuPPh}_3)\text{-}$

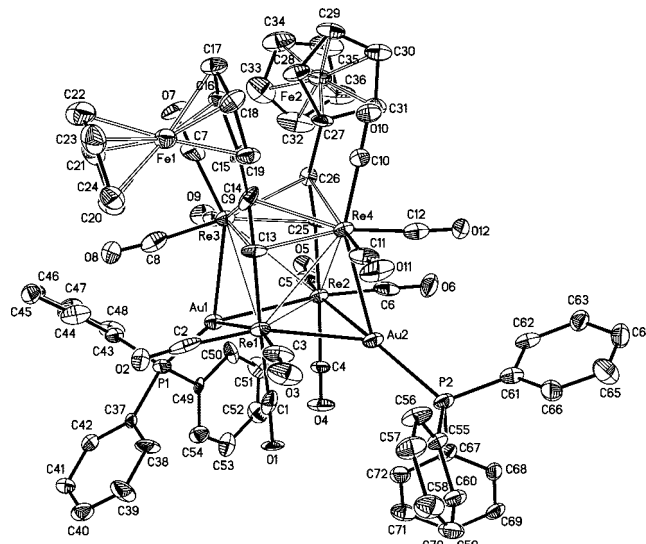


Figure 1. Molecular structure of **1** showing 30% probably ellipsoids. Selected bond lengths (Å) are as follow: Re(1)–Re(2) 3.047(1), Re(1)–Re(3) 3.308(1), Re(1)–Re(4) 3.241(1), Re(2)–Re(3) 3.309(1), Re(2)–Re(4) 3.290(1), Au(1)–Re(1) 2.823(1), Au(1)–Re(2) 2.848(1), Au(1)–Re(3) 2.896(1), Au(2)–Re(1) 2.839(1), Au(2)–Re(2) 2.860(1), Au(2)–Re(4) 2.900(1), Re(1)–C(13) 2.06(2), Re(2)–C(25) 2.01(2), Re(3)–C(13) 2.41(2), Re(3)–C(14) 2.41(2), Re(4)–C(13) 2.30(2), Re(4)–C(14) 2.51(2), Re(3)–C(25) 2.35(2), Re(3)–C(26) 2.40(2), Re(4)–C(25) 2.30(2), Re(4)–C(26) 2.54(2), C(13)–C(14) 1.35(2), C(25)–C(26) 1.20(2).

$(\text{CO})_9]^-$ (2.840(1), 2.845(1), and 2.826 Å).¹⁰ In **1** each of the four rhenium atoms is coordinated to three terminal CO groups. Finally, the cluster contains two μ_3 -ferrocenylalkynyl ligands symmetrically coordinated within the cavity of the wings, with C(13) and C(25) α -carbon atoms bound to the hinge atoms Re(1) and Re(2), respectively. The alkyne carbons C(13)–C(14) and

(7) (a) Koridze, A. A.; Kizas, O. A.; Petrovskii, P. V.; Kolobova, N. E.; Mikheeva, G. M. *Dokl. Akad. Nauk SSSR* **1987**, 293, 117. (b) Koridze, A. A.; Kizas, O. A.; Petrovskii, P. V.; Ezernitskaya, M. G.; Lokshin, B. V. *Metalloorg. Khim.* **1988**, 1, 1237. (c) Hardcastle, K. I.; Deeming, A. J.; Nuel, D.; Powell, N. I. *J. Organomet. Chem.* **1989**, 375, 217. (d) Koridze, A. A.; Yanovsky, A. I.; Struchkov, Yu. T. *J. Organomet. Chem.* **1992**, 441, 277. (e) Koridze, A. A.; Zdanovich, V. I.; Sheloumov, A. M.; Lagunova, V. Yu.; Petrovskii, P. V.; Peregudov, A. S.; Dolgushin, F. M.; Yanovsky, A. I. *Organometallics* **1997**, 16, 2285. (f) Strelets, V. V.; Zdanovich, V. I.; Lagunova, V. Yu.; Sheloumov, A. M.; Koridze, A. A. *Russ. Chem. Bull.* **1997**, 46, 1721. (g) Sheloumov, A. M.; Koridze, A. A.; Dolgushin, F. M.; Starikova, Z. A.; Ezernitskaya, M. G.; Petrovskii, P. V. *Russ. Chem. Bull., Int. Ed.* **2000**, 49, 1292. (h) Koridze, A. A.; Zdanovich, V. I.; Sheloumov, A. M.; Dolgushin, F. M.; Ezernitskaya, M. G.; Petrovskii, P. V. *Russ. Chem. Bull., Int. Ed.* **2001**, 50, 2441. (i) Bruce, M. I.; Skelton, B. W.; White, A. H.; Zaitseva, N. N. *J. Organomet. Chem.* **2002**, 650, 188. (j) Bruce, M. I.; Skelton, B. W.; Smith, M. E.; White, A. H. *Aust. J. Chem.* **1999**, 52, 431.

(8) (a) Yip, J. H. K.; Wu, J.; Wong, K. Y.; Yeung, K. W.; Vittal, J. J. *Organometallics* **2002**, 21, 1612. (b) Yip, J. H. K.; Wu, J.; Wong, K. Y.; Ho, K. P.; Pun, C. S. N.; Vittal, J. J. *Organometallics* **2002**, 21, 5292. (c) Berry, J. F.; Cotton, F. A.; Murillo, C. A. *Organometallics* **2004**, 23, 2503. (d) Xu, G. L.; De Rosa, M. C.; Crutchley, R. J.; Ren, T. J. *Am. Chem. Soc.* **2004**, 126, 3728. (e) Xu, G. L.; Crutchley, R. J.; De Rosa, M. C.; Pan, Q. J.; Zhang, H. X.; Wang, X.; Ren, T. J. *Am. Chem. Soc.* **2005**, 127, 13354. (f) Kuo, C. K.; Chang, J. C.; Yeh, C. Y.; Lee, G. H.; Wang, C. C.; Peng, S. M. *Dalton Trans.* **2005**, 3696. (g) Albinati, A.; Fabrizi de Biani, F.; Leoni, P.; Marchetti, L.; Pasquali, M.; Rizzato, S.; Zanello, P. *Angew. Chem., Int. Ed.* **2005**, 44, 5701.

(9) (a) Churchill, M. R.; Amoh, K. N.; Wasserman, H. J. *Inorg. Chem.* **1981**, 20, 1609. (b) Lee, K. W.; Pennington, W. T.; Cordes, A. W.; Brown, T. L. *J. Am. Chem. Soc.* **1985**, 107, 631. (c) Nubel, P. O.; Wilson, S. R.; Brown, T. L. *Organometallics* **1983**, 2, 515. (d) Kesz, H. D.; Bau, R.; Churchill, M. R. *J. Am. Chem. Soc.* **1967**, 89, 2775.

(10) Beringhelli, T.; Ciani, G.; D'Alfonso, G.; De Madle, V.; Freni, M. *J. Chem. Soc., Chem. Commun.* **1986**, 735.

C(25) - C(26) are connected to the wing-tip Re(3) and Re(4) atoms via an η^2 -bonding mode. The bridge bonds associated with these η^2 -interactions are somewhat asymmetric (Re(3)–C(13) = 2.41(2) Å, Re(3)–C(14) = 2.41(2) Å, Re(4)–C(13) = 2.30(2) Å, Re(4)–C(14) = 2.51(2) Å, Re(3)–C(25) = 2.35(2) Å, Re(3)–C(26) = 2.40(2) Å, Re(4)–C(25) = 2.30(2) Å, Re(4)–C(26) = 2.54(2) Å) differing by as much as 0.1 Å. Thus, each alkynyl ligand donates five electrons, and **1** is a 64e cluster. Complex **1** is the first example of a butterfly organometallic cluster with two $\mu_3\text{-}\eta^1\text{:}\eta^2\text{:}\eta^2$ -alkynyls symmetrically bridging the open M...M edge.

Butterfly clusters are usually associated with 62 metal-plus-ligand electrons, and dihedral angles varying within a wide range are sensitive to changes in electron density resulting from ligand donation. An elongation of one or more intermetallic distances and flattening of the metallic core are characteristic of electron-rich butterfly clusters. For example, in the 64e cluster $\text{Ru}_4(\mu\text{-PPh}_2)(\text{CO})_{13}(\mu\text{-}\eta^2\text{-C}\equiv\text{CBu})$,¹¹ the Ru_4 core is very flattened (the dihedral angle is equal to 176.93°), and two Ru–Ru bonds are significantly elongated (3.157(1) and 3.197(1) Å) as compared to the average value of the Ru–Ru distance found for $\text{Ru}_3(\text{CO})_{12}$ (2.8555(4) Å).^{12a} The dihedral angle between triangular Re(1)–Re(2)Re(3) and Re(1)Re(2)Re(4) wings is rather narrow, 73.2°, as compared to those for other butterfly clusters.

It is evident that an elongation of four Re–Re distances in **1** should result from electron excess in this complex. The narrow dihedral angle observed for **1** can be rationalized by the tightening effect of two multisite coordinated alkynyl ligands.

The ¹³C NMR of **2** in the carbonyl region shows three resonances at 195.92, 187.91 and 185.11 ppm in a relative intensity of 1:1:2. This indicates that in solution complex **2** has a plane of symmetry which makes the carbonyl groups on the two Re atoms equivalent. According to the solid state structure of **2** this should not be the case because the alkynyl ligand is η^1 bound to one Re atom and η^2 bound to the other in a σ - π bonding mode. However, σ - π interchange of bridging ligands is a well-known process in this type complexes and apparently in the case of **2** this is a particularly facile process owing to the presence of two equivalent electron pairs on the μ -alkynyl ligand.¹³ On the other hand, complex **1** shows four carbonyl resonances at 198.89, 191.23, 188.74, and 185.82 ppm in a relative intensity of 1:1:2:2, entirely consistent with symmetrical structure observed in the solid state. Significantly, the resonances at 188.74 and 191.23 are slightly broadened at ambient temperature indicating the onset of axial-radial (localized) exchange at the wing tip Re atoms. It is well-known that axial-radial exchange at the wing tip metal atoms of butterfly clusters occurs at somewhat lower temperatures than at the hinge metal atoms.^{12b,c}

Electrochemistry of 1, 2, and 3. In the cyclic voltammetric (CV) response on a glassy carbon electrode (GC) of a $\text{CH}_2\text{Cl}_2/0.1 \text{ M} [\text{NBu}_4]\text{PF}_6$ solution of **3** at 0.2 V s^{−1} scan rate (ν), two

oxidation processes are observed. The first peak couple ($E^{\circ'} = 0.00 \text{ V vs Fc/Fc}^+$) is diffusion controlled (the plots of i_p vs $\nu^{1/2}$ and i_p vs concentration of depolarizer are linear and go through the origin of the axes), electrochemically reversible (the peak-to-peak separation, $\Delta E_p = E_{p,a} - E_{p,c}$ is ca. 70 mV, and it is independent of ν in the whole experimentally used range 0.05–1.50 V s^{−1}), and chemically reversible (the anodic to cathodic peak ratio is unity at each scan rate).^{14,15} These features are compatible with the usual characteristics provided by a ferrocene-centered chemically and electrochemically reversible 1e oxidation. The second oxidation peak ($E_p = +1.30 \text{ V vs Fc/Fc}^+$ at 0.2 V s^{−1}), is an electrochemically reversible and chemically irreversible 1e oxidation (no reduction peak at any V) and can be ascribed to the AuPPh_3 moiety. If this peak is traversed, the chemical reversibility of the ferrocene-centered oxidation decreases, as testified by the decrease of the $i_{p,c}/i_{p,a}$ peak ratio. This means that the oxidation of the gold moiety influences also the stability of the ferrocenium cation. The chemical reversibility is completely restored at $\nu > 0.80 \text{ V s}^{-1}$.

In the CV response on a GC electrode of a $\text{CH}_2\text{Cl}_2/0.1 \text{ M} [\text{NBu}_4]\text{PF}_6$ solution of **2** at 0.2 V s^{−1}, the chemically and electrochemically reversible 1e oxidation of the Fc moiety is present once again ($E^{\circ'} = +0.490 \text{ V vs Fc/Fc}^+$). In addition an ill-defined series of oxidation processes are also observed at more positive potentials ($E > +0.75 \text{ V}$). For comparison with the behavior of **3**, we can assume that these oxidations are centered on the gold moiety. These oxidations quickly alter the surface of the solid electrode and will no longer be discussed. In fact, these peaks are compatible with absorption peaks overlapped to diffusion-controlled gold fragment oxidations. In the negative sweep, a reduction is observed ($E_p = -2.29 \text{ V vs Fc/Fc}^+$ at 0.2 V s^{−1}). This reduction process is chemically irreversible, since no associated reoxidation peak could be found even at scan rates as high as 1.50 V s^{−1}. In the reverse scan, a small peak is observed at $E_p = -1.70$ at 0.2 V s^{−1}, attributable to the reoxidation of fragment product(s). The breadth of the reduction peak at -2.29 V measured at the half-width ($E_p - E_{p/2}$) is 67 mV, close to 1e Nernstian (fast electron transfer) behavior. The plot of i_p vs $\nu^{1/2}$ is linear through the origin, confirming the diffusion-controlled behavior. The plot of E_p vs $\log \nu$ gives a slope of 45 mV, indicating that the 1e reduction is followed by a moderately fast, first-order chemical decomposition (EC mechanism).^{14,15} Because the peak is slightly higher than those of the ferrocene oxidation, we can presume that some electrogenerated product is reduced at the same potential increasing the total peak current. The reduction peak at -2.29 V may be ascribed to the Re moiety, by comparison with the redox behavior of compound **3**.

Figure 2 shows the CV response on a GC electrode of a $\text{CH}_2\text{Cl}_2/0.1 \text{ M} [\text{NBu}_4]\text{PF}_6$ solution of **1** at 0.2 V s^{−1}. Its overall appearance is not very different from that of compound **2**. In this case we also observe the ill-defined Au-centered oxidations at $E > 1.0 \text{ V}$ and a Re-centered 1e reduction peak (D'' , $E_p = -2.39$ at 0.2 V s^{−1}), both having the electrochemical characteristics of the similar peaks in **2**. The breadth of peak D'' ($E_p - E_{p/2}$) is higher than that observed for **2**; this prompted us to confirm that the electron transfer rate is slower, that is, we are in the presence of important structural rearrangements following

(11) Carty, A. J.; MacLaughlin, S. A.; Van Wagner, J.; Taylor, N. J. *Organometallics* **1982**, *1*, 1013.

(12) (a) Churchill, M. R.; Hollander, F. J.; Hutchinson, J. P. *Inorg. Chem.* **1977**, *16*, 2655. (b) Johnson, B. F. G.; Lewis, J.; Aime, S.; Milone, L.; Osella, D. *J. Organomet. Chem.* **1982**, *233*, 247. (c) Koridze, A. A.; Sheloumov, A. M.; Dolgushin, F. M.; Yanovsky, A. I.; Struchkov, Yu. T.; Petrovskii, P. V. *J. Organomet. Chem.* **1997**, *536–537*, 381.

(13) (a) Koridze, A. A.; Kizas, O. A.; Kolobova, N. E.; Petrovskii, P. V. *Izv. Akad. Nauk SSSR, Ser. Khim.* **1984**, 472; *Bull. Acad. Sci. USSR, Div. Chem. Sci.* **1984**, *33*, 437 (Engl. Transl.). (b) Koridze, A. A.; Kizas, O. A.; Petrovskii, P. V.; Kolobova, N. E.; Struchkov, Yu. T.; Yanovsky, A. I. *J. Organomet. Chem.* **1988**, *338*, 81. (c) Nubel, P. O.; Brown, T. L. *Organometallics* **1984**, *3*, 29. (d) Beatty, S. T.; Bergman, B.; Rosenberg, E.; Dastrù, W.; Gobetto, R.; Milone, L.; Viale, A. *J. Organomet. Chem.* **1999**, *593–594*, 226.

(14) Bard, A. J.; Faulkner, L. R. *Electrochemical Methods. Fundamentals and Applications*, 2nd ed.; J. Wiley: New York, 2001.

(15) Zanello, P. *Inorganic Electrochemistry. Theory, Practice and Applications*; Royal Society of Chemistry: London, 2003.

(16) (a) Štěpnička, P.; Trojan, L.; Kubišta, J.; Ludvík, J. *J. Organomet. Chem.* **2001**, *637–639*, 291. (b) Back, S.; Gossage, R. A.; Lang, H.; van Koten, G. *Eur. J. Inorg. Chem.* **2000**, 1457.

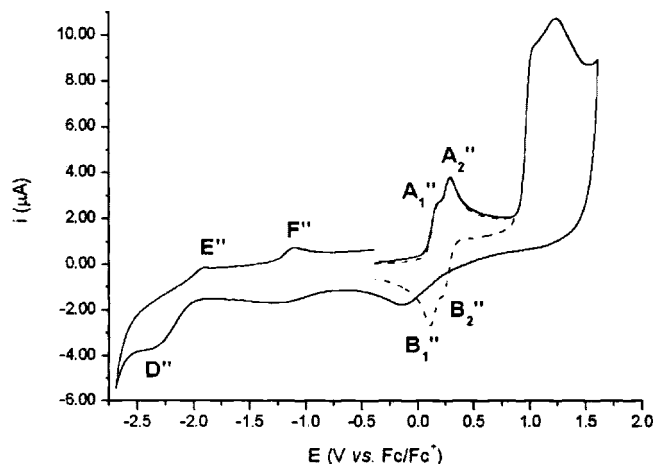


Figure 2. Cyclic voltammogram of 1.1 mM in CH_2Cl_2 ; 0.1 M TBAPF₆, WE = GC, $\nu = 0.2 \text{ V s}^{-1}$.

Table 1. Formal Electrode Potentials of Ferrocenylalkynyl Compounds in CH_2Cl_2

compound	$E^{\circ'}(0/1+)$ (V vs Fc/Fc ⁺)	ref.
Fc-C≡C-H	0.11	16a
3 ^a	0.00	this work
2	0.49	this work
1	0.156 [0,0/0,1+], 0.265 [0,1+/1+,1+]	this work

^a This compound has been earlier studied in THF solution.^{16b}

the redox step to stabilize the electrogenerated anion. Furthermore, as for **2**, in the reverse scan small peaks (E'' at $E_p = -1.90 \text{ V}$ and F'' at $E_p = -1.10 \text{ V}$ measured at 0.2 V s^{-1}) are observed, attributable to the reoxidation of fragment product(s). However, in this compound, the pattern of the ferrocene-centered oxidation is more complicated. In fact, two redox couples are observed at $E^{\circ'} = +0.156$ (peak couple A₁''/B₁'') and $+0.265 \text{ V}$ (peak couple A₂''/B₂''), respectively.

Table 1 summarizes the electrochemical (oxidation) data together with that of Fc-C≡C-H for comparison.^{16a} These data illustrate that the -C≡C-H moiety acts as an electron-withdrawing group, as far as Fc-C≡C-H is oxidized less easily than Fc-H. The fragment AuPPh₃ pushes electrons to the Fc moiety and its effect counterbalances that of the ethynyl group ($E^{\circ'} = 0.00 \text{ V}$ vs Fc/Fc⁺). The effect of the Re framework is more electron-withdrawing in **2** than in **1**, but, in general, in the presence of an electronic delocalization, oxidations or reductions are shifted to more favorable potentials.

It is known that for a compound consisting of two similar redox centers linked by a ligand or a metal bridge, two extreme cases can be considered:¹⁷ (i) there is no electronic interaction between the two redox cores (the group between the two redox centers is an insulator). The $E^{\circ'}$ values for the redox processes differ by a small statistical factor, ca. 36 mV at 298 K, and in polarography/CV a single wave/peak (having the slope of a one-electron transfer, but the height of a two-electron process) is observed (*valence-trapped systems*);^{17–19} (ii) there is complete charge delocalization over the two centers (the group between the two redox centers is a conductor). The difference between the $E^{\circ'}$ values of the two redox processes ($\Delta E^{\circ'}$) may be more than 700 mV and in polarography/CV two well-resolved wave/peaks (each corresponding to one electron) are observed

(*valence delocalized systems*).^{20,21} Between these extremes, a large number of organometallic compounds exists having weakly interacting redox centers, giving lower $\Delta E^{\circ'}$ values. Compound **1** falls into this category since the two ferrocene oxidations are separated by 109 mV. It is rather difficult to estimate the two formal potentials from the CV trace because they partially overlap. In order to measure the $E^{\circ'}$ values better, a mathematic transformation making use of the deconvolution principle has been performed. The *semi-integral* of the CV current, generated by the operator $d^{-1/2}/dt^{-1/2}$ transforms a peak-shaped linear/cyclic potential sweep response into an S-shaped polarographic curve, the half-wave potential, $E_{1/2}$, being coincident with the formal electrode potential, $E^{\circ'}$. The flex point, corresponding to $E^{\circ'}$, can be defined for a peak by evaluating its first derivative.

By comparing the one electron oxidation potentials of complexes **1** and **2**, $+0.156$ and $+0.49 \text{ V}$ respectively, it is evident that each ferrocenyl group in **1** bears more electron density than the Fc-group in **2** (in other words, the cluster $\text{Re}_4(\text{AuPPh}_3)_2(\text{CO})_{12}$ withdraws less electron density from the two Fc-groups, than the cluster $\text{Re}_2(\text{AuPPh}_3)(\text{CO})_8$ from the ferrocenyl group). Therefore, we may conclude that the relative shielding of the protons of the substituted cyclopentadienyl in **1** and **2** is the result of magnetic anisotropy and not electronic effects.

Near Infrared Spectra. NIR spectra are extremely informative with regard to evaluating electronic communication between two metal atoms in different oxidation states. While neutral complexes do not absorb in the NIR region, in the spectra of mixed-valence complexes with pronounced electronic interaction between the metal centers, a broad intense band is observed. This band is associated with intervalence charge transfer (so-called IVCT band) from one metal center to the other via a bridging ligand. The appearance of broad low-energy absorptions with high extinctions, that are narrower than predicted by the Hush theory, is indicative of electronic communication in the molecule.²² Parameters of the bands (transition energy, extinction, band half-width) allow one to estimate a delocalization coefficient α . According to the classification proposed by Robin and Day,²³ there exist three classes of molecular conductors which differ according to the degree of interaction between metallic centers of the molecule. Substances, where there is no interaction between metallic centers ($\alpha \approx 0$) belong to Class **I** conductors (*valence-trapped systems*). Substances with a significant interaction between two metallic centers ($0.707 > \alpha > 0$), in which charge separation between metallic centers of different valence is maintained belong to Class **II** conductors; and substances with a large interaction degree ($\alpha = 0.707$), in which there is no more charge separation between metallic centers, belong to Class **III** molecular conductors (*valence-delocalized systems*).

There are numerous data in the literature concerning intramolecular charge transfer in organometallic complexes, where two or more metallic centers are connected via an organic ligand capable of being electron density conductors (for example, a chain of sp-hybridized atoms). However, there are only a few examples of mixed-valence complexes, where the intramolecular electronic communication occurs through transition metal clusters.^{8,24}

(20) McCleverty, J. A.; Ward, M. D. *Acc. Chem. Res.* **1998**, *31*, 841.

(21) Glöckle, M.; Kaim, W. *Angew. Chem., Int. Ed.* **1999**, *38*, 3072.

(22) Hush, N. S. *Prog. Inorg. Chem.* **1967**, *8*, 391.

(23) Robin, M. B.; Day, P. *Advan. Inorg. Chem. Radiochem.* **1967**, *10*, 247.

(24) Adams, R. D.; Qu, B.; Smith, M. D.; Albright, T. A. *Organometallics* **2002**, *21*, 2970.

(17) Creutz, C. *Prog. Inorg. Chem.* **1983**, *30*, 1.

(18) Richardson, D. E.; Taube, H. *Coord. Chem. Rev.* **1984**, *60*, 107.

(19) Crutchley, R. J. *Adv. Inorg. Chem.* **1999**, *41*, 273.

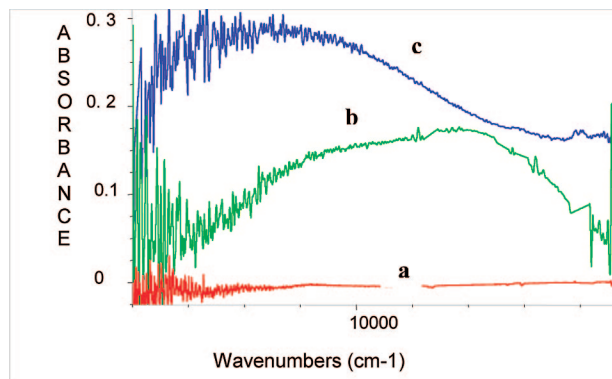


Figure 3. NIR spectra of complexes **1** and **1**⁺: (a) neutral **1** in CH₂Cl₂; (b) **1**⁺ in CH₂Cl₂; (c) **1**⁺ in acetone.

The NIR spectra were measured for the neutral complexes **1** and **3** and their mixed-valence monocationic forms **1**⁺ and **3**⁺ in CH₂Cl₂ and acetone solutions. The spectra are presented in Figures 3 and 4. The neutral complexes **1** and **3** have no absorption in the NIR region (Figures 3a and 4a). The monocationic mixed-valence complexes **1**⁺ and **3**⁺ were obtained by gradual addition of a [FcAc]BAR'₄ (Ar' = 3,5-(CF₃)₂C₆H₃) solution to a solution of neutral complexes. In the NIR spectra of monocationic complex **1**⁺ in CH₂Cl₂ solution, broad absorption bands appear (Figure 3b). The maximum extinction was obtained with a 1:1 complex/oxidant molar ratio indicating that 1e oxidation was achieved. The bands in the NIR spectra of **1**⁺ show significant solvatochromism: on going from methylene chloride to acetone, instead of the two bands observed for complex **1**⁺ in CH₂Cl₂ solution, one much broader band is observed in acetone (Figure 3c) which is shifted 1700 cm⁻¹ to higher frequency. These broad low-energy absorption bands in the spectra of mixed-valence complexes, which are absent in the spectra of corresponding neutral compounds, can be assigned to intervalence electron transfer (IVCT bands) and are characteristic of electronic coupling between two metal centers of different valence. The presence of several IVCT bands happens rather frequently and can originate from several causes, for example, from the possibility of electron transfer from several filled molecular orbitals or from level splitting due to spin-orbital interactions.

Using the Hush methodology,²² the parameters for intervalence electron transfer were estimated. The band half-height width was estimated by the formula

$$\Delta\nu_{1/2 \text{ calc}} = \sqrt{2310\nu_{\text{max}}}$$

and compared to the half-height width in the experimental spectra.

The energy of electron coupling between the two iron centers of different valence was estimated by the formula

$$V^2(\text{cm}^{-1}) = 4.2 \cdot 10^{-4} \cdot \nu_{\text{max}} \epsilon_{\text{max}} \Delta\nu_{1/2} / d_{\text{MM}}^2$$

The delocalization parameter α was estimated by the formula

$$\alpha = \sqrt{4.2 \cdot 10^{-4} \epsilon_{\text{max}} \Delta\nu_{1/2} / \nu_{\text{max}} d_{\text{MM}}^2}$$

where ν_{max} = position of the IVCT band in cm⁻¹, ϵ_{max} = extinction, $\Delta\nu_{1/2}$ = band half-height width, d_{MM} = the distance between two metal centers of different oxidation states.

The difficulty in the use of the above equations is the value of the d_{MM} parameter, which represents an effective distance between localized donor and acceptor charge centers. It is

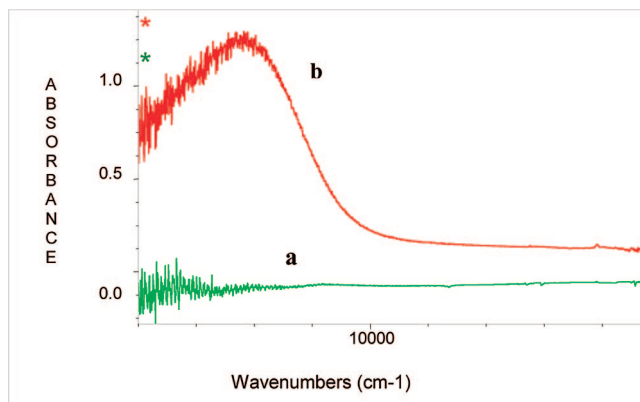


Figure 4. NIR spectra of complexes **3** and **3**⁺: (a) neutral **3** in CH₂Cl₂; (b) **3**⁺ in CH₂Cl₂.

usually taken as the through-space geometrical distance between the metal sites.²⁵ The d_{MM} parameter value (7.43 Å) was taken from the X-ray data for the neutral complex **1** as the direct distance between the iron atoms. This value is approximate because in solutions the complex is conformationally flexible and the Fe–Fe distance can vary for different conformations.

The parameters of the NIR bands for complexes **1**⁺ and **3**⁺ are presented in Table 2.

The data presented in Table 2 show that for complexes **1**⁺ and **3**⁺, there is a significant electronic coupling between the metal centers in different oxidation state. Solvatochromism observed for complex **1**⁺ confirms the charge-transfer origin of the bands in the NIR spectra. The values of the energy of the electron transfer and the α values obtained for complexes **1**⁺ and **3**⁺ indicate that they belong to Class II conductors, that is, there is high degree of intramolecular charge transfer between the metal centers, but the charge separation still exists.

Complex **1**⁺ has no linear chain of unsaturated bonds capable of transporting electron density; however, a transition metal atom can also play the role of a transporting bridge. There are examples in the literature, where electronic coupling was observed in complexes with spacers including a chain of transition metal atoms, but these spacers have structures close to linear. For example, significant electronic communication in complexes *trans*-(FcC_{2n})Ru₂(Y-DMBA)₄(C_{2m}Fc) ($n, m = 1, 2$; DMBA = *N,N'*-dimethylbenzamidinate, Y = H, OMe) via the chain including two ruthenium atoms has been reported.^{8e} In the NIR spectra, intense and quite narrow IVCT bands were observed for complexes with the Fe...Fe distances of 11.6–16.6 Å. We observed intramolecular electronic coupling in the iridium ferrocene-based pincer complex {Ir(CO)[^t-BuP,C,P^{Fe}]}PF₆ of nonlinear structure.²⁶ Besides, through-space electronic communication is also quite probable. O'Hare et al.⁵ observed a through-space electron transfer for mixed-valence monocationic bisferrocenyl species bound via saturated bridges (CMe₂, SiMe₂, GeMe₂), in which the Fe...Fe distances were 4.5–7.5 Å. The authors observed weak broad bands in the NIR spectra (ϵ 134, 87, 62, respectively). The most significant interaction was observed for the complex with the CMe₂ bridge where the iron atoms were arranged at the shortest distance. In this case, the energy of the electronic interaction (V) was equal to 200 cm⁻¹ and the α value was equal to

(25) Launay, J. P. *Chem. Soc. Rev.* **2001**, 30, 386.

(26) Kuklin, S. A.; Sheloumov, A. M.; Dolgushin, F. M.; Ezernitskaya, M. G.; Peregodov, A. S.; Petrovskii, P. V.; Koridze, A. A. *Organometallics* **2006**, 25, 5466.

Table 2. Parameters of the IVCT Bands in the NIR Spectra of Complexes 1⁺ and 3⁺

complex	ν (cm ⁻¹)	ν (nm)	ϵ (M ⁻¹ cm ⁻¹)	$\Delta\nu_{1/2\text{obs}}$ (cm ⁻¹)	$\Delta\nu_{1/2\text{calc}}$ (cm ⁻¹)	$\Delta\nu_{1/2\text{obs}}/\Delta\nu_{1/2\text{calc}}$	V (cm ⁻¹)	V (eV)	α
1 ⁺ in CH ₂ Cl ₂	10200	9980	446	2936	4200	0.7	318.8	0.04	0.03
	7600	1316	523	2453					
1 ⁺ in acetone	11900	840	294	6430	5240	1.23	413.7	0.05	0.035
3 ⁺ in CH ₂ Cl ₂	12100	826	776	2022	5290	0.38	454.7	0.056	0.119

0.03. Weak intramolecular electronic through-space interaction was observed for [Fc₃CH]⁺.²⁷ The energy of this interaction was only 24 cm⁻¹, α was 0.004.

We suppose that in the case of **1**, electron transfer is possible from one iron atom to the other *via* the metallic core or through space. The value of the interaction parameter α obtained for complex 1⁺ (0.03) coincides with that obtained for through-space a interaction in monocationic bisferrocenyl complexes with the CMe₂ bridge,⁵ though the IVCT bands for these complexes are much weaker than those for complex 1⁺. We believe that the NIR spectra for complex 1⁺ cannot provide evidence for the mechanism of electronic transfer, but they unambiguously indicate that electronic communication between two iron centers of different valence does exist. This fact seems very promising in view of tuning this interaction by purposeful chemical design of these types complexes.

In complex 3⁺ two metal atoms in different oxidation state are linked via the C≡C fragment, which provides the possibility for electron transfer from Au to Fe⁺ atoms. The interaction between the metal centers is confirmed by the NIR spectra (Figure 4). The parameters of the IVCT band for complex 3⁺ are presented in Table 2. It is seen that extinction of the IVCT band for complex 3⁺ is markedly higher than that for complex 1⁺. The distance between the metal atoms (6.21 Å) was taken from the X-ray crystallographic data for a related compound {[η²-(Ph₃P)AuC≡CFc]Cu(μ-Cl)}₂.²⁸ For compound 3⁺, the value of the α parameter is about four times higher (0.12) as compared to that for complex 1⁺ indicating that the intramolecular electron transfer in this compound is much stronger.

Concluding Remarks

In summary, the novel heteronuclear digold-tetrarhenium cluster **1** with an unusual structure having two equivalent ferrocenylethynyl ligands has been synthesized and it exhibits significant electronic communication between the ferrocenyl groups, which is seldom observed for cluster complexes. The unusual geometry of complex **1**, with its unique spacial arrangement of two redox-active groups (the relatively short distance between two ferrocene units) allows the investigation of the possible through-space intramolecular electronic interaction in this and related systems. In the future we will study factors that influence the degree of electronic communication between redox active ferrocene units.

Experimental Section

General Considerations. Reactions were run in an argon atmosphere and isolation of the product was carried out in air. Chromatographic purifications were carried out with silica gel 60, 70–230 mesh (Lancaster). The solvents were dried and degassed by standard methods under an argon atmosphere. Deuterated solvents were degassed with argon. Commercially available reagents

were used as received. Complex Re₂(AuPPh₃)(CO)₈(μ-C≡CFc) (**2**) was prepared as described in the literature.^{7h}

¹H and ³¹P{¹H} NMR spectra were recorded at 400.13, and 161.98 MHz, respectively, using a Bruker AMX-400 NMR spectrometer. ¹³C{¹H} NMR spectra were recorded at 125 MHz on a Varian NMR Systems 500 MHz NMR spectrometer. ¹H and ¹³C{¹H} NMR chemical shifts are reported in parts per million downfield from tetramethylsilane. ¹H NMR chemical shifts were referred to the residual hydrogen signal of the deuterated solvents. ³¹P NMR chemical shifts are reported in parts per million downfield from H₃PO₄ and referred to an external 85% solution of phosphoric acid in D₂O. NIR spectra were recorded on a JSD-205 Fourier Transform spectrometer. Elemental analyses were performed at the A.N. Nesmeyanov Institute of Organoelement Compounds of RAS.

An Autolab PGSTAT12 electrochemical analyzer (Eco Chemie, Utrecht, The Netherlands) interfaced to a personal computer running GPES 4.9 electrochemical software was used for the cyclovoltammetric measurements. A standard three-electrode cell was designed to allow the tip of the reference electrode (Ag/AgCl) to closely approach the working (a glassy carbon disk, diameter 0.1 cm, sealed in epoxy resin), and the auxiliary (a Pt wire) electrodes. All measurements were carried out under nitrogen in CH₂Cl₂ solutions containing 0.1 M [NBu₄]PF₆ as supporting electrolyte and the metal clusters 1.0 × 10⁻³ M. All potentials are reported vs the Fc/Fc⁺ couple, added to the solutions as an internal standard.

Synthesis of Re₄(AuPPh₃)₂(CO)₁₂(μ₃-C≡CFc)₂ (1**).** Complex Re₂(AuPPh₃)(CO)₈(μ-C≡CFc) (**2**) (90 mg) was dissolved in benzene (40 mL) and the solution was refluxed for 2.5 h, resulting quantitative transformation of **2** into complex **1**, indicated by ³¹P NMR spectroscopy. After cooling, the solvent was removed under vacuum, and the residue was chromatographically purified on a column with silica gel. The major orange-red fraction was eluted with a petroleum ether-CH₂Cl₂ (2:1) mixture. Red crystals of the complex **1** were obtained by crystallization from a hexane-CH₂Cl₂ mixture; the yield was 85% (76 mg).

¹H NMR (CDCl₃): δ 4.16 (s, 10H, C₅H₅) 4.55 (t, 4H, C₅H₄, J = 2.0 Hz), 4.98 (t, 4H, C₅H₄, J = 2.0 Hz), 7.40–7.60 (m, 30H, C₆H₅). ¹³C{¹H} NMR (CDCl₃): δ 185.8 (s, 4CO), 188.7 (s, 4CO), 192.2 (s, 2CO), 198.9 (s, 2CO). ³¹P{¹H} NMR (CDCl₃): δ 90.4 (s, 2P). IR (CH₂Cl₂): 2010 (vs), 1997 (vs), 1992 (vs), 1933 (vs), 1916 (m) cm⁻¹ (ν_{CO}). Anal. calcd for C₇₅H₅₄Au₂Fe₂O₁₃P₂Re₄: C, 35.77; H, 2.00. Found: C, 35.73; H 2.00.

X-Ray Diffraction Study. Red plate-like crystals of **1** were grown from acetone solution. Crystal data for 1 Me₂CO: C₇₅H₅₄Au₂Fe₂O₁₃P₂Re₄, M = 2475.55, triclinic, space group $P\bar{1}$, at 140(1) K, a = 12.636(3), b = 15.155(4), c = 22.624(6) Å, α = 72.464(5), β = 81.748(6), γ = 65.852(6)°, V = 3768(2) Å³, d_{calc} = 2.182 g/cm³ for Z = 2, μ = 10.748 mm⁻¹. Intensities of 14688 independent reflections and cell parameters were measured at 140(1) K with a Bruker SMART 1000 CCD diffractometer²⁹ using Mo K α radiation (λ = 0.71073 Å, graphite monochromator, ω -scan with 0.3° step and 20s per frame exposure, 2θ < 52°, semiempirical absorption correction from equivalents,³⁰ min/max transmission factors 0.064/0.525). The structure was solved by direct methods and refined by the full-matrix least-squares technique against F^2 in the anisotropic approximation. Hydrogen atoms were placed geometrically and included in the structure factor calculation in the riding motion approximation. The refinement converged to wR_2 = 0.1603 and GOF = 1.019 for all independent reflections

(27) Delgado-Pena, F.; Talham, D. R.; Cowan, D. O. *J. Organomet. Chem.* **1983**, 253, C45.

(28) Lang, H.; Kocher, S.; Bach, S.; Rheinwald, G.; van Koten, G. *Organometallics* **2001**, 20, 1968.

($R_1 = 0.0710$ was calculated against F for 7833 observed reflections with $I > 2\sigma(I)$). All calculations were carried out using SHELXTL-97.³¹ The rather high R values and the residual electron density found near the heavy atoms may be due to the presence of disordered solvent molecules. These were not included in the final structure refinements.

Acknowledgment. Università del Piemonte Orientale is gratefully acknowledged for a financial support in the form of a travel grant to A.S. and E.R. (Fondo per la Cooperazione Internazionale). A.K. and E.R. acknowledge the support of the Civilian Defense Research Foundation for support of this work.

Supporting Information Available: Tables of complete distances and bond angles, atomic coordinates, and anisotropic thermal parameters for **1**. This material is available free of charge via the Internet at <http://pubs.acs.org>.

OM800589G

(29) SMART V5.051 and SAINT V5.00, Area detector control and integration software; Bruker AXS Inc.: Madison, WI, 1998.

(30) Sheldrick, G. M. SADABS, Program for Empirical Absorption Correction of Area Detector Data; University of Gottingen: Germany, 1996.

(31) Sheldrick, G. M. SHELXTL-97 V5.10; Bruker AXS Inc.: Madison, WI, 1997.